Theoretical study of polar interfaces of the (122) Sigma =9 grain boundary in cubic SiC

1991 J. Phys.: Condens. Matter 3 7555

(http://iopscience.iop.org/0953-8984/3/39/003)

J. Phys.: Condens. Matter 3 (1991) 7555–7573. Printed in the UK

Theoretical study of polar interfaces of the {122} $\Sigma = 9$ grain boundary in cubic SiC

M Kohyama†, S Kose† and R Yamamoto‡

† Glass and Ceramic Material Department, Government Industrial Research Institute, Osaka, 1-8-31, Midorigaoka, Ikeda, Osaka 563, Japan

‡ Research Center of Advanced Science and Technology, University of Tokyo, 4-6-1, Komaba, Meguro-ku, Tokyo 153, Japan

Received 1 May 1991

Abstract. The polar and non-polar interfaces of grain boundaries in the zinc blende structure can be defined by the stoichiometry in the interface region, and it is possible to construct two polar interfaces and one non-polar interface for a symmetrical-tilt grain boundary for which the interface comprises the polar surfaces. The atomic and electronic structures of polar interfaces of the {122} $\Sigma = 9$ grain boundary in SiC have been examined using the self-consistent tight-binding method coupled with the supercell technique, and they have been compared with our previous results for the non-polar interface. In the present atomic models consisting of a zigzag arrangement of 5–7 units, which is consistent with an HREM image, one polar interface contains the C—C wrong bonds and another polar interface contains the Si—Si wrong bonds, although the non-polar interface contains both types of wrong bonds. The present calculated results indicate that as well as the non-polar interface the respective polar interfaces are possibly stable without the generation of any macroscopic electrostatic fields or excess free carriers, although the wrong bonds introduce localized states at the band edges and an increase in the electrostatic energy similar to the non-polar interface. This is because the atomic charges in SiC are mainly caused by the bond polarization and the wrong bonds do not generate any extra carriers or deep states in SiC, unlike ionic solids or heterovalent compound semiconductors. The calculated energy of formation of the pair of polar interfaces is rather smaller than that of the non-polar interfaces, because the energy increase caused by bond distortions is smaller in the polar interfaces, which contain only one type of wrong bond. By using the calculated binding energies, the relative stability of the polar and non-polar interfaces of the {122} $\Sigma = 9$ boundary in SiC has been analysed thermodynamically as a function of the atomic chemical potentials. The calculated thermodynamic potentials of the interfaces indicate that either one or the other polar interface is always more stable than the non-polar interface for the allowable ranges of the atomic chemical potentials. There is a general discussion of the stability of the polar interfaces in SiC and in compound semiconductors.

1. Introduction

Significant advances have been made in the understanding of atomic and electronic structures of grain boundaries in elemental semiconductors such as Si and Ge [1, 2]. From various observations [3–6] and theoretical calculations [7–10] it has been shown that the frequently observed tilt grain boundaries are constructed by arranging structural units such as five-membered rings and seven-membered rings and are electrically non-active because of dangling-bond reconstruction at interfaces.

0953-8984/91/397555 + 19 $03.50

As the next step it is of much interest to investigate the grain boundaries in compound semiconductors or covalent ceramics such as GaAs, AlN or SiC. In such grain boundaries, further complexity should exist such as the wrong bonds between like atoms, the stoichiometry at interfaces or the polarity of the two grains, which are all different from the grain boundaries in elemental semiconductors. Since the early crystallographic models and discussion by Holt [11] it has only been recently that experimental information about the atomic structures of grain boundaries in compound semiconductors or covalent ceramics, such as GaAs or SiC, have been obtained using the high-resolution electron microscopy (HREM) technique [12–15]. Nowadays, it is of much importance to understand theoretically the atomic and electronic structures of such grain boundaries.

There has been increasing interest in SiC as high-performance ceramics or high-temperature devices and it is of great importance to investigate the structures and properties of grain boundaries or interfaces in SiC from a microscopic viewpoint. In our previous paper [16], which is referred to as paper I in the present paper, we have performed the first theoretical approach to the $\{122\}\ \Sigma = 9$ boundary in cubic SiC. We have constructed an atomic model from a HREM image by Hiraga [14], which consists of a zigzag arrangement of five-membered and seven-membered rings (5–7 units) in a similar fashion to the same boundary in Si or Ge [3, 4, 6]; the model contains the Si—Si and C—C wrong bonds repeated alternately at the interface. We call this model a non-polar interface. Polar and non-polar interfaces can be defined by the stoichiometry in the interface region in the present paper, as will be specified in the following section. In paper I, from the calculation using the self-consistent tight-binding (SCTB) method [17] coupled with the supercell technique, it has been shown that the non-polar interface of the $\{122\}\ \Sigma = 9$ boundary can be stable in SiC and that the wrong bonds cause no deep states in the gap, although the increase in the electrostatic energy caused by the wrong bonds is a large part of the boundary energy and the wrong bonds introduce the wrong-bond localized states at the band edges.

As mentioned in paper I it is possible to construct two other types of interface model only by inverting the polarity of one of the two grains of the non-polar interface. These two models contain only the C—C wrong bonds or the Si—Si wrong bonds, respectively, as the wrong bonds at the interface, and are called polar interfaces. In these polar interfaces, problems related to the polar character and the stoichiometry of the interfaces, as well as the polar surfaces of compound semiconductors [18, 19] or the polar interfaces in semiconductor heterojunctions [20, 21], seem to occur, in addition to the problem of the wrong bonds.

In the present paper we examine the atomic and electronic structures of the polar interfaces of the $\{122\}\ \Sigma = 9$ boundary in SiC using the same theoretical method as used in paper I. The results are compared with those for the non-polar interface. This is the first theoretical approach to the polar interfaces of boundaries in compound semiconductors or covalent ceramics from an atomic and electronic level. As we will see the present results indicate the possibility of the presence of the respective polar interfaces of the $\{122\}\ \Sigma = 9$ boundary in SiC without generating any macroscopic electrostatic fields or excess free carriers. In order to examine the relative stability of the polar and non-polar interfaces it is necessary to perform a thermodynamic analysis using the thermodynamic potential [22] as a function of the atomic chemical potentials, because the polar interfaces are non-stoichiometric systems. As will be shown the present analysis indicates that either one or the other polar interface is always more stable than the non-polar interface for the allowable ranges of the atomic chemical potentials.

This paper is organized as follows. In section 2 we first specify the relation between the polar and non-polar interfaces and the paratwin and orthotwin in the zinc blende

structure, and present crystallographic conditions for the occurrence of polar and non-polar interfaces in symmetrical-tilt grain boundaries and antiphase boundaries. Then we specify the three types of interface models; models of two polar and one non-polar interfaces of the {122} $\Sigma = 9$ boundary in SiC. In section 3 the theoretical method used in the present paper, the SCTB method coupled with the supercell technique, is explained. Special consideration is needed in treating polar interfaces in the supercell method, because both types of polar interfaces must be included in one unit cell. In sections 4 and 5 the results of the supercell calculations are presented and analysed. In section 6 the relative stability of the polar and non-polar interfaces is analysed thermodynamically using the present calculated results. In section 7 there is a general discussion of the stability of polar interfaces in SiC and in compound semiconductors.

2. Polar and non-polar interfaces in the zinc blende structure

In the general description of grain boundaries in the zinc blende structure the relation between the polarities of the two grains is necessary, in addition to a geometric description of the grain boundaries such as that for the diamond structure. With respect to the one type of boundary in the diamond structure four types of boundaries can be defined in the zinc blende structure because of the two directions of the polarity of the respective grains. About the symmetrical-tilt grain boundaries or twins, three types of boundaries can be defined, because two of the four types of boundaries are equivalent in these cases. These are the two paratwins and one orthotwin as discussed by Holt [11]. Here, we use a term, twin, as a general symmetrical tilt grain boundary. A paratwin, or inversion twin, is a symmetrical tilt grain boundary where the polarity of the two grains displays mirror symmetry to each other with respect to the interface. One additional paratwin can be constructed by inverting the polarity of both the two grains of the paratwin. An orthotwin, or upright twin, is constructed by inverting the polarity of one of the two grains of the paratwins. It should be noted that the inversion of the polarity of both of the two grains of the orthotwin generates an equivalent orthotwin. The relation between the paratwin and the orthotwin can also be explained by the additional rotation of one of the two grains by 180° in the case of the ⟨011⟩ tilt grain boundaries and by 90° in the case of ⟨001⟩ tilt grain boundaries as shown by Holt [11].

On the other hand, the polar and non-polar interfaces of the grain boundaries or antiphase boundaries in binary compounds can be defined by the stoichiometry in the interface region without introducing any point defects, analogously to polar and non-polar surfaces. As pointed out by Sutton [23], any periodic boundaries in cubic binary compounds can be constructed either by two polar or two non-polar surfaces. Therefore, non-polar interfaces can be constructed with two non-polar surfaces or by anion-terminated and cation-terminated polar surfaces. Polar interfaces can be constructed with two anion-terminated polar surfaces or with two cation-terminated polar surfaces.

We think that the classification into polar and non-polar interfaces is important, as well as that into the paratwins and orthotwins. Polar interfaces are non-stoichiometric systems, and should have a problem of charge accumulation in ionic solids without introducing any point defects. In the case of compound semiconductors of the zinc blende structure, polar interfaces should contain one type of wrong bond or one type of excess wrong bond within the models where all the atoms are four-coordinated ones, although non-polar interfaces should either contain no wrong bonds or the same numbers of the two types of wrong bonds. This is a natural result of stoichiometry in the interface

region. This problem of polar interfaces in compound semiconductors should generate the problem of excess free carriers as discussed in section 7. It is not the case of isovalent compounds such as SiC as we will see.

The general conditions for the occurrence of polar and non-polar interfaces in symmetrical-tilt grain boundaries in the zinc blende structure and the relation between the polar and non-polar interfaces and the paratwins and orthotwins can be stated as follows. Within the models for symmetrical-tilt grain boundaries constructed from two ideal surfaces without the introduction of any point defects, paratwins constructed from polar surfaces generate polar interfaces and paratwins constructed from non-polar surfaces generate non-polar interfaces. In addition, orthotwins always generate non-polar interfaces. In other words, for symmetrical-tilt grain boundaries for which the interface consists of polar surfaces such as {111} or {122}, two polar interfaces and one non-polar interface can be constructed, which correspond to two paratwins and one orthotwin. Symmetrical-tilt grain boundaries for which the interface consists of non-polar surfaces should have only non-polar interfaces.

Here the polar and non-polar surfaces are defined by the stoichiometry of the atomic layer at the surface, and the general condition for the non-polar surface is that the Miller indices have the form of {odd, odd, even} as pointed out by Sutton [23].

The present conditions for the polar and non-polar interfaces in symmetrical-tilt grain boundaries can be easily understood by considering the difference in the polarity of the surfaces of the two grains in the paratwin and the orthotwin. By applying several simple models of the symmetrical ⟨011⟩ and ⟨001⟩ tilt grain boundaries in Si [24] to paratwins and orthotwins in the zinc blende structure, we have found that the present conditions are applicable, at least in the models constructed from two ideal surfaces without the introduction of any point defects.

In the case of antiphase boundaries it can be said that those for which the interface is a polar plane generate polar interfaces, and vice versa, which is similar to the case of paratwins. This condition is similar to that pointed out by Holt in [25], where type 1 and type 2 correspond to non-polar and polar interfaces, respectively. However, it seems that the condition of the non-polar plane considered by Sutton is more general and preferable to that given in [25].

The most simple example of a symmetrical tilt grain boundary in the zinc blende structure is the $\{111\}\,\Sigma = 3$ boundary [13]. As discussed above, two polar and one non-polar interfaces can be constructed, which correspond to two paratwins and one orthotwin. The non-polar interface is constructed by both cation-terminated and anion-terminated (111) surfaces and contains ordinary anion–cation bonds at the interface. The polar interfaces are constructed by both anion-terminated (111) surfaces or by both cation-terminated (111) surfaces and should contain only anion–anion wrong bonds or only cation–cation wrong bonds at the interfaces.

For the $\{122\}\,\Sigma = 9$ boundary in the zinc blende structure, two polar interfaces and one non-polar interface can be similarly constructed by the {122} polar surfaces as shown in figure 1. In these models the interface structures consist of a zigzag arrangement of 5–7 units and dangling bonds are reconstructed in a similar fashion to the atomic structure of the same boundary in Si or Ge [3, 4, 6]. At the polar interfaces only one type of wrong bond is introduced at the interfaces, as shown in figures 1(*a*) and 1(*b*), although both types of wrong bonds are repeated alternately at the non-polar interface in figure 1(*c*). In this paper, the polar interface containing the anion–anion wrong bonds shown in figure 1(*a*) is called 'N-type', and the polar interface containing the cation–cation wrong bonds shown in figure 1(*b*) is called 'P-type', according to [13].

It is clear that the polar interfaces in figure 1 can be constructed by inverting one of the two grains of the non-polar interface. The non-polar interface only has a mirror symmetry with respect to the {011} plane and is expressed as *pm*. The polar interfaces have a glide plane symmetry with respect to the interface in addition to the {011} mirror symmetry, and are expressed as $p2_1^1ma'$. From the argument about symmetry the polar interfaces permit only a compression or a dilatation normal to the interface, although the non-polar interface permits a rigid-body translation along the ⟨411⟩ direction in addition to that normal to the interface [16].

As mentioned in paper I, Hiraga [14] has obtained the HREM images of the {122} Σ = 9 boundary in chemical vapour-depositioned (CVD) cubic SiC, and Hagège *et al* [26] have shown by image simulation that atomic models consisting of a zigzag arrangement of 5–7 units, such as those in figure 1, can explain the HREM image. However, the polarity of the grains has not been determined experimentally and it has not been examined which interface model in figure 1 should really exist in SiC. Following the non-polar interface approach in paper I we deal with the remaining two polar interface models of the {122} Σ = 9 boundary in SiC in the present paper.

3. The theoretical method

In this paper we use the SCTB method [17, 27] coupled with the supercell technique, which was used as well in paper I. The tight-binding theories have been shown to be quite useful for calculations of grain boundaries in elemental semiconductors [7–10]. For solids with both covalent and ionic characters such as SiC, it is necessary to incorporate the effects of self-consistent charge redistribution and electrostatic interactions. The SCTB method can deal with these effects properly, and is capable of calculating the electronic structure, the total energy and the atomic forces sufficiently rapidly for the lattice relaxation of extended defects.

The precise description of the SCTB method in the *k*-space formulation has already been given in [16, 17]. The tight-binding Hamiltonian is expressed using a local-orbital basis set, where one s and three p valence atomic orbitals per atom are included. The two-centre integrals of the Hamiltonian are expressed by assuming an r^{-2} dependence on the interatomic distance r and using the universal parameters [27]. Charge transfer effects are included self-consistently in the on-site elements of the Hamiltonian [27] as

$$E_{i\alpha} = E^0_{i\alpha} + U_i(Q_i - Z_i) + P_i + f_{i\alpha}. \tag{1}$$

The first term is the orbital energy of the neutral atom i. The second term expresses the change in the intra-atomic electrostatic potential. U_i is an average of the intra-atomic Coulomb integrals of the valence electrons of the atom i. Z_i and Q_i are the charge of the ion core and the self-consistent valence electron occupancy of the atom i, respectively. The third term is the interatomic electrostatic potential for an electron located on the atom i. This is given by a sum of contributions from the effective atomic charges of all the atoms except the atom i using the effective interatomic electrostatic function, which includes the effect of charge overlap for short distances. The fourth term is the non-orthogonality correction, which includes the effect of the overlap matrix elements between basis atomic orbitals to first order.

By solving the Schrödinger equation self-consistently the band structure energy E_{bs} is given as a sum of occupied eigenenergies. The total energy E_{tot} is found by subtracting

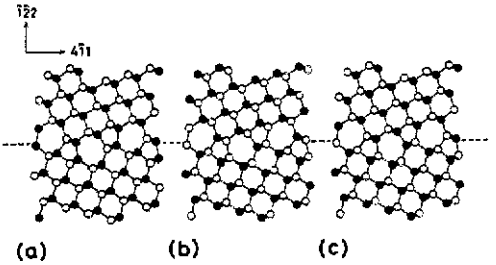

Figure 1. Atomic models of the {122} $\Sigma = 9$ grain boundary in the zinc blende structure: (*a*), N-type polar interface; (*b*), P-type polar interface; (*c*), non-polar interface. Atomic positions are projected along the [011] axis. The open and closed circles indicate the cation and anion atoms, respectively, which correspond to Si and C atoms, respectively, in SiC.

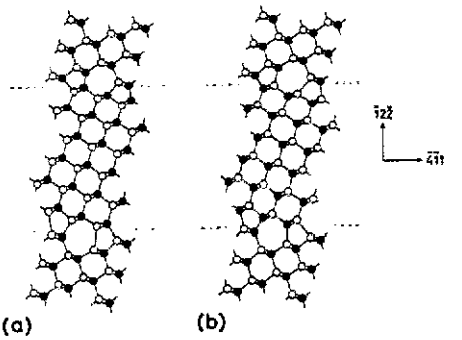

Figure 2. Unit cells of the supercell configuration for the {122} $\Sigma = 9$ grain boundary in the zinc blende structure. (*a*) The 80-atom cell for the polar interfaces. The two types of polar interfaces are stacked alternately. (*b*) The 80-atom cell for the non-polar interface. Two equivalent non-polar interfaces are stacked. Broken lines indicate the positions of the interfaces.

the doubly counted electron–electron electrostatic energy and adding the ion–ion electrostatic energy. The binding energy E_B, which is the difference between the value of E_{tot} of the system and that of the free atoms, can be written as a sum of four terms, E_{pro}, E_{Mad}, E_{ov} and E_{cov}. E_{pro} contains the promotion energy, the energy gain by electron transfer between different atoms and the change in the intra-atomic electrostatic energy between electrons. E_{Mad} is the interatomic electrostatic energy, which is a sum of interactions between effective atomic charges, $Q_i - Z_i$. E_{ov} is the overlap energy caused by the non-orthogonality correction in equation (1), which generates the repulsive interaction between atoms. E_{cov} is the covalent energy and contains only the contribution from the interatomic covalent bonding.

Atomic forces are also given very easily via the Hellmann–Feynman theorem [28] as well as other tight-binding methods, and lattice relaxation can be carried out easily. In this paper we use the same parameters and functional forms as those used in paper I, which can reproduce the basic properties of cubic SiC, Si and C [17].

Unlike the non-polar interface in paper I there are two problems in the supercell calculation of the polar interfaces. These problems are similar to those that occur for the polar surfaces of compound semiconductors [18, 19]. Firstly, it is necessary to stack both types of polar interfaces, the N-type and the P-type interfaces, alternately, in order to construct a supercell configuration with periodicity normal to the interface. Thus, the unit cell of the supercell must contain two inequivalent polar interfaces as shown in figure 2, although the two equivalent interfaces are included in the unit cell for the non-polar interface. This is a geometric restriction. It is not possible to deal with the respective polar interfaces separately in the supercell method.

Secondly, the polar interfaces should be regarded as non-stoichiometric systems, where one extra C layer or Si layer is inserted at the interface as compared with the ordinary alternate stacking of Si and C {122} atomic layers as shown in figures 1 and 2. For non-stoichiometric systems it is not possible to define the total change in energy with respect to the bulk SiC crystal. In order to analyse the relative stability of systems with different stoichiometry, it is necessary to consider the thermodynamic potential [22] as

a function of the atomic chemical potentials of the two species as well as in the case of the polar surfaces of compound semiconductors [18, 19]. For this purpose it is necessary to obtain the total energies or the binding energies of the respective polar interface regions in order to estimate the thermodynamic potential as we shall see in section 6. This seems to be difficult in band calculations for the above supercell containing both types of polar interfaces.

In the present paper we, firstly, calculate the total energy, the stable atomic configuration and the electronic structure for the above-mentioned supercell containing both types of polar interfaces in one unit cell, and the results are compared with those of the non-polar interface [16]. The present supercell has the perfect stoichiometry and it is possible to define the total energy of the cell with respect to bulk SiC. In addition, it should be possible to examine the structures and properties of the respective polar interfaces using the present type of supercell if there are no significant charge transfers nor interactions between the two types of polar interfaces in the supercell. As shown in the following section it has been found that this condition can be almost satisfied for large cells.

With respect to the above second point, there is a possibility that the calculation of the binding energies of the respective polar interface regions can be accomplished in the SCTB method. Here, it should be noted that the respective energy terms of the binding energy, E_{pro}, E_{Mad}, E_{ov} and E_{cov} can be given for respective atoms in the unit cell. This is apparent for the former three terms as shown in our previous paper [17] and it is possible to partition the term E_{cov} into the respective atoms in the unit cell, because this term can be expressed as a sum of partial bond orders multiplied by the Hamiltonian matrix elements [17]. Thus, in the present paper, we have calculated the above energy terms and the differences from those in bulk SiC for the respective atoms in the supercell. By dividing the unit cell into the two non-stoichiometric interface regions it is possible to calculate the binding energies of the respective polar interface regions as sums of the energy terms of atoms. This is the special advantage of the SCTB method. For example, by dividing the unit cell in the middle between the two interfaces, the N-type interface region containing 36 Si and 37 C layers and the P-type interface region containing 36 Si and 35 C layers can be determined in the 144-atom cell. Of course, it should be noted that the sums of the energies for the interface regions can be interpreted physically only when the total charge neutrality is preserved for the respective interface regions. As we shall see this is approximately attained for large cells.

4. Energy, atomic structure and atomic charges

The lattice relaxation has been performed for the supercell containing both types of polar interfaces. The present supercell structure is orthorhombic and belongs to the point group C_{2v}. Both 80-atom and 144-atom cells have been used in order to examine the dependence on the cell size as used in paper I. The distances between the two interfaces in these two supercells are about 15 and 26 Å, respectively. The optimum initial rigid-body translation between the two grains was determined by iterating the lattice relaxation of the 80-atom cell for various initial translations. The same initial translation was used for the lattice relaxation of the 144-atom cell. The special k-points and all the conditions in the Ewald sums, in the self-consistent iteration and in the relaxation procedure are the same as those in paper I.

Table 1. Calculated energy values of the polar and non-polar interfaces of the {122} $\Sigma = 9$ grain boundary in cubic SiC. The energy increases per supercell against the values in the perfect crystal are shown. Each supercell for the polar interface contains both types of polar interfaces, and each supercell for the non-polar interface contains the two equivalent non-polar interfaces. E_{gb} is the interfacial energy per unit area for one stoichiometric non-polar interface.

	Polar interface		Non-polar interface [16]	
	80-atom cell	144-atom cell	80-atom cell	144-atom cell
ΔE_{pro} (eV/cell)	−1.404	−1.411	−1.785	−1.785
ΔE_{Mad} (eV/cell)	3.685	3.682	4.022	4.021
ΔE_{ov} (eV/cell)	7.691	7.566	7.756	7.645
ΔE_{cov} (eV/cell)	−5.448	−5.321	−4.915	−4.808
ΔE_{B} (eV/cell)	4.524	4.516	5.079	5.072
E_{gb} (J m^{-2})	—	—	1.427	1.425

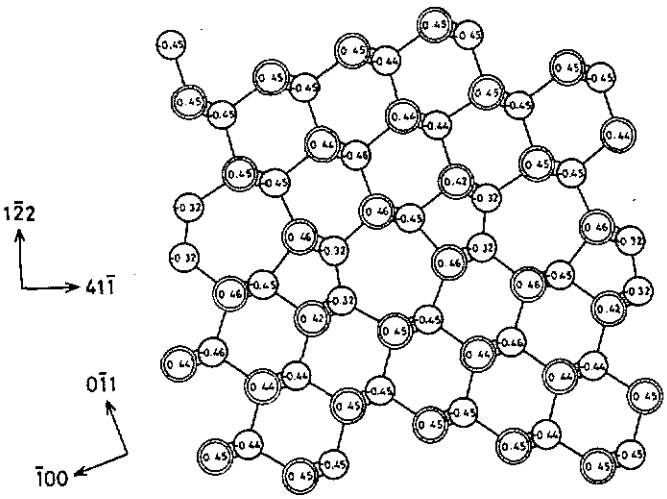

Figure 3. Relaxed atomic structure and atomic charges of the N-type polar interface of the {122} $\Sigma = 9$ grain boundary in cubic SiC. Atomic positions are projected along the [011] axis. The circles and the double circles indicate C atoms and Si atoms, respectively. The numbers inside the circles indicate the effective charges of the respective atoms, $-(Q_i - Z_i)$, expressed in units of e. Those in the perfect crystal are $\pm 0.45e$ [17].

Table 1 shows the calculated energy values for the supercell. These values are the increases in energy for the pair of polar interfaces as compared with bulk SiC. It should be noted that the respective energy terms do not have a great dependence on the cell size. The previously calculated values for the supercell containing the two equivalent non-polar interfaces [16] are also listed in table 1. Figures 3 and 4 show the relaxed atomic configurations and the calculated self-consistent atomic charges of the N- and P-type polar interfaces in the 144-atom cell. The differences in the atomic structures and charges near the interfaces between the two sizes of cells are negligibly small. The

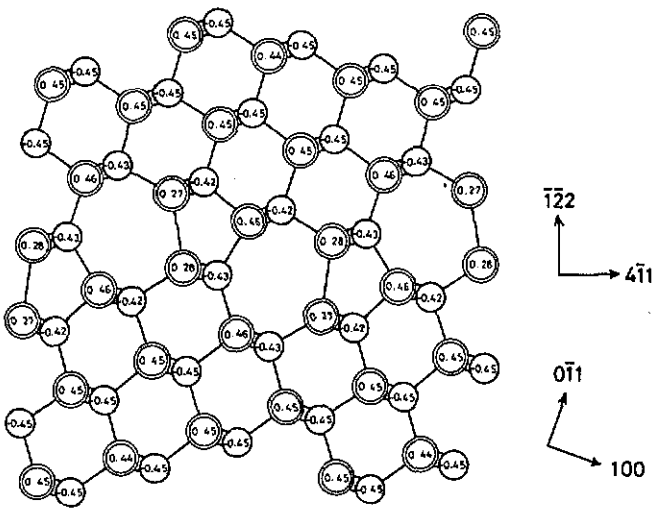

Figure 4. Relaxed atomic structure and atomic charges of the P-type polar interface of the {122} Σ = 9 grain boundary in cubic SiC.

optimum rigid-body translation is a compression of $0.013a_0[1\bar{2}2]$ for the N-type interface containing the C—C wrong bonds, and is a dilatation of $0.025a_0$ $[\bar{1}\bar{2}2]$ for the P-type interface containing the Si—Si wrong bonds. These are determined by measuring the distances between the centres of the grains in the relaxed supercell as compared with the distances in the ordinary stacking of the {122} atomic layers. The rigid-body translation for the non-polar interface is a dilatation of $0.005a_0$ $[\bar{1}2\bar{2}]$ and a translation of $0.01a_0[\bar{4}\bar{4}1]$ parallel to the interface [16].

About the present self-consistent charge distribution, it can be said that there is no charge accumulation at the polar interfaces and no macroscopic electrostatic fields in the supercell. If there is charge accumulation at the interfaces in the present supercell, the resulting periodic electrostatic fields between the interfaces would generate large deviations of interatomic electrostatic potentials P_i near the interfaces, and this should depend on the distance between the interfaces in the supercell. However, the present deviations of P_i near the interfaces are in the same range as those found in the non-polar interface, and the charge distributions and P_i near the interfaces are almost the same in both the 80-atom and 144-atom cells. In addition ΔE_{Mad} does not depend on the cell size, as shown in table 1.

It can be said that there is no charge transfer between the two polar interfaces in the present supercell. The charge neutrality is preserved for the respective non-stoichiometric interface regions containing one extra C or Si atomic layer. For example, the electron transfer from the N-type interface region containing 36 Si and 37 C atomic layers to the P-type interface region containing 36 Si and 35 C atomic layers in the 144-atom cell is only $0.0007e$.

The present results of no charge accumulation or charge transfer between the interfaces can be understood by considering the origin of the atomic charges in SiC. It can be said that the atomic charges in SiC are mainly caused by the bond polarization because the valence numbers of Si and C are the same. For example, the magnitudes of atomic charges of the atoms at the wrong bonds are not so different from three quarters of the

bonds in bulk SiC, because these atoms possess three heteropolar bonds and one homopolar bond as compared with the four heteropolar bonds of the ordinary atoms. Thus, it can be stated that the charge neutrality should be approximately preserved for the respective bonds. Of course, it is important that the present wrong bonds in SiC do not cause any extra carriers or deep states, as will be shown in the following section; unlike the case of heterovalent compound semiconductors [29]. Otherwise the artificial charge transfer between the two types of polar interfaces should exist in the supercell.

As shown in figures 3 and 4 charge fluctuations exist at the interfaces, especially around the wrong bonds. These fluctuations of the atomic charges and of the interatomic electrostatic potentials P_i are localized near the interfaces, and these are almost like the values in the bulk near several of the {122} atomic layers apart from the interfaces. For example, the deviations of the atomic charges larger than $\pm 0.01e$ and the deviations of P_i larger than ± 0.1 eV are localized in the 5–7 units. Of course, this is correlated with the structural disorder, such as bond distortions localized near the interfaces. We conclude that the present supercell is sufficiently large that the effects of disorder at the interfaces are well screened. It is also true that there are no significant interactions between the two types of polar interfaces in the present supercell. This is also guaranteed by the near independence of the calculated energy terms and the electronic structure on the cell size as shown in table 1, and as shown in the following section.

The present results of no charge accumulation, or any significant charge transfer or interactions between the two interfaces in the supercell, indicate that the structures and properties of the respective polar interfaces in the supercell calculated here can be regarded as of general validity. They also indicate the possibility of the presence of the respective polar interfaces without the generation of any macroscopic fields. By considering the limit of an infinitely large distance between the two types of polar interfaces in the supercell, it can be stated that the respective polar interfaces possibly exist solely in SiC in the same state as in the present supercell.

The charge fluctuations at the respective interfaces, shown in figures 3 and 4, are somewhat larger in the P-type interface than in the N-type interface. Excess electronic charges of $0.17e$ and $0.18e$ exist at the Si—Si wrong bonds in the P-type interface as compared with the electrons in bulk SiC, although the deviations at the C—C wrong bonds in the N-type interface are reductions of $0.12e$ and $0.13e$. These, relatively many, electrons at the Si—Si wrong bonds at the P-type interfaces are compensated by the neighbouring atoms in the 5–7 units that contain fewer electrons as compared with those in bulk SiC.

Concerning the fluctuations of the interatomic electrostatic potentials P_i there are no dipole shifts at the present polar interfaces because of the symmetry of the interface structures. However, it should be noted that an interface dipole shift exists at the non-polar interface in our previous calculation, although this is mentioned as the opposite direction of the shifts of P_i on both sides of the interface in paper I [16]. This has been found to correspond to the interface dipole shift by reanalysing the previous results. As pointed out by Sutton [23] it is possible that an interface consisting of two inequivalent polar surfaces has an interface dipole. The value of the dipole shift is about 0.3 eV, which has been estimated from the shifts of P_i in the atomic layers on both sides of the 5–7 units at the non-polar interface.

For the case of the relaxed structure of the N-type interface in figure 3 the C—C wrong bond is 2.5% longer than that in bulk diamond. The bond angle deviations range from -21.8 to $19.7°$, and the bond length deviations of normal Si—C bonds range from -2.5 to 2.1%. For the relaxed structure of the P-type interface in figure 4 the Si—Si

wrong bond is 1.9% shorter than that in bulk Si. The bond angle deviations range from −13.1 to 21.1°, and the bond length deviations of normal Si—C bonds range from −2.1 to 1.4%. Large deviations are localized at and around the 5–7 units in both the interfaces. In the non-polar interface [16] the C—C wrong bond is 3.8% longer than that in bulk diamond, the Si—Si wrong bond is 4.3% shorter than that in bulk Si, the bond angle deviations range from −23.1 to 24.1° and the bond length deviations of normal Si—C bonds range from −2.5 to 2.2%. The bond angle and bond length deviations are smaller at the polar interfaces rather than those in the non-polar interface, and the numbers of largely wrong bond lengths and bond angles are smaller in the polar interfaces, especially at the P-type interface. This is because the polar interfaces containing only one type of wrong bonds are more favourable for lattice relaxation including rigid-body translations rather than the non-polar interface containing both types of wrong bonds.

One of the most interesting features of the present results is that the total energy per supercell, in other words the formation energy of the pair of polar interfaces, is rather smaller than that of the pair of non-polar interfaces as shown in table 1. This is caused by the above-mentioned relaxed structures. As shown in table 1 the energy increase mainly caused by the bond distortions at the polar interfaces, $\Delta E_{ov} + \Delta E_{cov}$, is much smaller than that at the non-polar interfaces. However, the increase in the electrostatic and transfer energies, $\Delta E_{pro} + \Delta E_{Mad}$, at the polar interfaces is somewhat larger than that at the non-polar interfaces.

The energy values for the polar interfaces in table 1 can be analysed by using the atomic structures and charges shown in figures 3 and 4 and the energy terms of respective atoms as follows. The value of ΔE_{pro} is negative, and the large reduction of the intra-atomic electrostatic energies $\frac{1}{2}U_i Q_i^2$ caused by the reduction in the number of electrons at the C—C bonds is most responsible for this, although this reduction in energy is counterbalanced by the increase in the same terms at the Si—Si bonds, by the increase in s–p mixing at the C—C bonds, and by the decrease of the energy gain of electron transfer caused by the wrong bonds, as well as at the non-polar interface. As compared with the value of ΔE_{pro} of the non-polar interface shown in table 1 the absolute value for the polar interfaces is slightly smaller. This seems to be caused by the positive values of ΔE_{pro} of the respective atoms in the 5–7 units at the P-type interface except for the Si—Si bonds, because these atoms are deficient in electrons as mentioned above.

ΔE_{Mad} is positive as shown in table 1 and is caused by the presence of the wrong bonds as well as at the non-polar interfaces. The values of ΔE_{Mad} of the respective atoms are 0.382 eV and 0.396 eV for the C atoms at the C—C wrong bond, and 0.443 eV and 0.453 eV for the Si atoms at the Si—Si wrong bond. These are in a similar range to those at the non-polar interface, and form 91% of the total value of ΔE_{Mad}. As mentioned above the fluctuations of atomic charges and P_i are concentrated around the interfaces, and individual atomic values of ΔE_{Mad} larger than ±0.05 eV are localized in the 5–7 units.

As compared with the value of ΔE_{Mad} of the non-polar interface the present total value of ΔE_{Mad} of the polar interfaces is rather smaller, as shown in table 1. It seems that this is caused by the relative stabilization of E_{Mad} for the atoms around the N-type interface that are accompanied by a compression of the N-type interface, as compared with the dilatation in the P-type interface and in the non- polar interface. For example, the total value of ΔE_{Mad} of the atoms in the 5–7 units at the N-type interface except for the wrong bonds is fairly small compared with that at the P-type interface.

$\Delta E_{ov} + \Delta E_{cov}$ is considered to be caused mainly by the bond distortions around the interfaces. As shown in table 1 this value of the polar interfaces is 2.245 eV, and is smaller

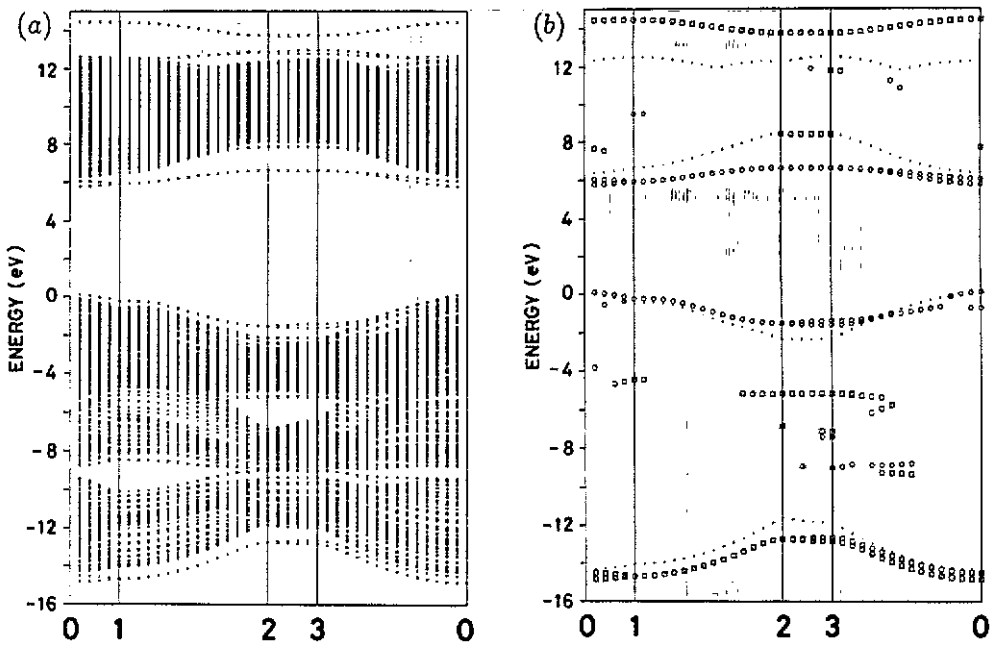

Figure 5. (*a*) The energy band structure of the polar interfaces of the $\{122\}\,\Sigma = 9$ grain boundary in cubic SiC. All the eigenvalues of the 144-atom cell containing both types of polar interfaces are plotted. Points 0, 1, 2 and 3 in the Brillouin zone are $(0, 0, 0)$, $(\pi/R_1, 0, 0)$, $(\pi/R_1, \pi/R_2, 0)$ and $(0, \pi/R_2, 0)$, respectively, where $R_1 = (3\sqrt{2}/2)a_0$ and $R_2 = (\sqrt{2}/2)a_0$. (*b*) Wrong-bond localized states. The squares indicate the states for which the probability that an electron is located on the C atoms of the C—C wrong bonds at the N-type interface exceeds 25%. The circles indicate the states for which the probability that an electron is located on the Si atoms of the Si—Si wrong bonds at the P-type interface exceeds 25%. The dotted curves indicate the projected band structure of the perfect crystal.

than that of the non-polar interface, 2.837 eV, although the values of $\Delta E_{\text{pro}} + \Delta E_{\text{Mad}}$ are comparable. This is caused by the relatively small bond length and bond angle distortions around the polar interfaces as mentioned above. It seems that another contribution is the energy reduction accompanied by the generation of the present C—C bond at the N-type interface, of which the length is nearer to that in bulk diamond than the C—C bond at the non-polar interface. In addition, the values of $\Delta E_{\text{ov}} + \Delta E_{\text{cov}}$ for the respective atoms are found to be frequently negative in the C atoms around the Si—Si wrong bonds at the P-type interface. This seems to be caused by the back bond strengthening against the weak Si—Si bonds, and is related to the reduction of the total value of $\Delta E_{\text{ov}} + \Delta E_{\text{cov}}$.

5. Electronic structure

Figure 5 shows the electronic structure of the polar interfaces. This has been calculated for the relaxed 144-atom cell containing both types of polar interfaces, and is shown along the lines in the plane with $k_z = 0$ in the orthorhombic Brillouin zone. We have

found that the difference between the electronic structures of the 80-atom cell and of the 144-atom cell is negligibly small.

The electronic structure of the pair of polar interfaces is similar to that of the non-polar interface in paper I. There are no deep states in the fundamental gap nor any free carriers. Many new states exist especially at the band edges as compared with the projected band structure of the perfect crystal, and most of these new states are the wrong-bond localized states as shown in figure 5(*b*) as well as at the non-polar interface. The bands at the top of the valence band and at the bottom of the conduction band are localized states at the Si—Si wrong bonds at the P-type interface. The bands at the bottom of the valance band and above the conduction band are localized states at the C—C wrong bonds at the N-type interface. Some of these states at the band edges are sharply localized, of which more than 90% of the contents are localized at the wrong bonds and the neighbouring atoms in the 5–7 units. In addition, localized states at the C—C wrong bonds at the N-type interface exist near the pseudogap within the valence band. States localized mainly at the 5–7 units of the N-type interface and those localized mainly at the similar units of the P-type interface exist at the lower edge of the conduction band around points 2 and 3 in figure 5(*a*). For all the above localized states, analogous states exist at the non-polar interface [16]. New types of states as compared with those at the non-polar interface are those localized mainly to the 5–7 units of the N-type interface, which exist at the upper edge of the conduction band in figure 5(*a*). In figure 5(*b*) the degeneracy of the wrong-bond localized states at the band edges is sometimes broken by interactions between the neighbouring wrong bonds at the polar interfaces, unlike the case of the non-polar interface.

It seems that the wrong bonds at the polar interfaces generate states similar to those at the non-polar interface, as obtained in paper I. It can be stated that the N- and P-type interfaces have electronic structures characterized by the C—C and Si—Si wrong-bond localized states, respectively. Additionally the 5–7 units of the two types of polar interfaces generate different localized states. As discussed in the preceding section, the present results for local electronic structures of the respective polar interfaces do not seem to depend on the present supercell condition, and should be regarded as general.

It should be noted that the wrong bonds in SiC do not generate extra carriers, unlike the oversaturated or undersaturated wrong bonds in heterovalent compound semiconductors [29], because both Si and C have four valence electrons. The mechanism of the occurrence of the wrong-bond localized states has already been analysed in paper I. The changes in the interatomic Hamiltonian matrix elements caused by the bond length deviations from the normal Si—C bonds in the wrong bonds are most responsible. The reason why the wrong bonds do not cause deep states, unlike the case in several compound semiconductors, is that the differences between the atomic levels of Si and C are not as large as those in several compound semiconductors.

Recently, Lambrecht and Segall [30] have calculated the total energy and electronic structure of the non-polar {011} antiphase boundary in cubic SiC using the LMTO method. As well as our previous and present results for the {122} $\Sigma = 9$ boundary, they have found that the electrostatic repulsion at the wrong bonds is a large part of the boundary energy, and found that the localized states caused by the Si—Si wrong bonds exist in the band gap. However, they found that these states are deep and are pushed up into the conduction band by lattice relaxation, causing a two-dimensional electron gas at the interface. This point is inconsistent with our results, although the density of the wrong bonds at the interface of the {011} antiphase boundary is fairly high as compared with the {122} $\Sigma = 9$ boundary. It should be noted that our results are consistent with the

calculations of antisite defects in cubic SiC, where the wrong bonds do not generate any deep states in the fundamental gap [31]. We think that the effects of the cell size and the method of lattice relaxation in their calculations should be examined in future. Of course, it is important to examine the position of the Si—Si wrong-bond localized states at the {122} $\Sigma = 9$ boundary in SiC more quantitatively in future.

6. Relative stability of the polar and non-polar interfaces

In this section we perform the thermodynamic analysis for the relative stability of the polar and non-polar interfaces of the {122} $\Sigma = 9$ boundary in SiC, in a similar fashion to the analyses performed for the polar surfaces of GaAs [18, 19] or the island formation of GaAs on Si [32]. For this purpose it is necessary to calculate the thermodynamic potential;

$$\Omega = E - TS - \sum_i n_i \mu_i. \tag{2}$$

This quantity is a measure of the stability of systems with different stoichiometries [22, 32]. In this relation E is the total energy, μ_i is the atomic chemical potential of the ith constituent, n_i is the total number of the ith constituent atoms and the sum is over all the constituents.

We suppose that the interface is in equilibrium with bulk SiC and appropriate elemental reservoirs, where the respective atoms can be exchanged and the chemical potential of a given atomic species is the same in all the phases. For the atomic chemical potentials, μ_{Si} and μ_C, the allowable ranges can be determined as discussed in [19]. The upper limits of the atomic chemical potentials are those of the bulk crystalline phases, μ_{Si}^{bulk} and μ_C^{bulk}. The equilibrium with bulk SiC leads to the relation

$$\mu_{Si} + \mu_C = \mu_{SiC}^{bulk} = \mu_{Si}^{bulk} + \mu_C^{bulk} - \Delta H \tag{3}$$

where ΔH is the heat of formation of SiC. Thus, the allowable ranges of the atomic chemical potentials and the difference $\Delta\mu = \mu_{Si} - \mu_C$ can be given as follows

$$\mu_{Si}^{bulk} - \Delta H \leqslant \mu_{Si} \leqslant \mu_{Si}^{bulk} \tag{4a}$$

$$\mu_C^{bulk} - \Delta H \leqslant \mu_C \leqslant \mu_C^{bulk} \tag{4b}$$

and

$$\mu_{Si}^{bulk} - \mu_C^{bulk} - \Delta H \leqslant \Delta\mu \leqslant \mu_{Si}^{bulk} - \mu_C^{bulk} + \Delta H. \tag{4c}$$

In principle, the bulk chemical potentials, μ_{Si}^{bulk}, μ_C^{bulk} and μ_{SiC}^{bulk} are given by the Gibbs free energy. However, as discussed in [19], for these values in condensed phases it is possible to use the approximate total energies per atom or atom pair at $T = 0$ K. Thus, we use the binding energies of bulk Si, bulk diamond and bulk SiC that were calculated in our previous paper [17], -4.63, -7.37 and -12.68 eV, respectively, which are the same as the experimental values. The value of ΔH is 0.68 eV. In addition, in the calculation of the thermodynamic potential of equation (2) we neglect the entropy term, TS, because this term should be approximately cancelled between different interfaces. For E we use the calculated binding energies of the respective interface regions, which are given as a sum of energy terms of atoms in the respective regions as mentioned in section 3. Here, it should be noted that the total energies are replaced by the binding

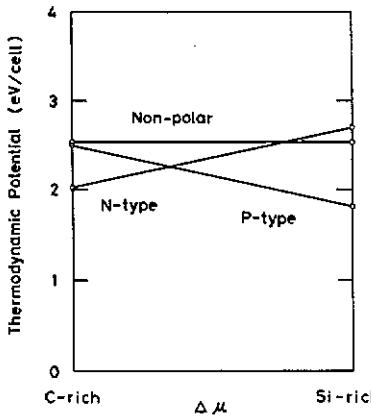

Figure 6. The thermodynamic potentials of the polar and non-polar interfaces of the {122} Σ = 9 grain boundary in cubic SiC as functions of the difference between the atomic chemical potentials for Si and C ($\Delta\mu = \mu_{Si} - \mu_C$). The lower limit of $\Delta\mu$ corresponds to $\mu_C = \mu_C^{bulk}$. The upper limit of $\Delta\mu$ corresponds to $\mu_{Si} = \mu_{Si}^{bulk}$.

energies from the free atoms in the present argument. This does not influence the result because this effect is totally cancelled out.

The thermodynamic potential Ω for the respective interfaces can be given as follows. For the stoichiometric non-polar interface, the sum of the atomic chemical potentials in equation (2) is equal to the binding energy of bulk SiC because of the condition expressed in equation (3). Thus, Ω is equal to the energy increase by the interface shown in table 1, which is 2.536 eV per unit cell of one interface regardless of the atomic chemical potentials. For the non-stoichiometric polar interfaces, Ω depends on the atomic chemical potentials, the allowable ranges of which are given in equation (4). By using the condition of equation (3), only one type of atomic chemical potential of the excess species is included in calculation of equation (2). For the C-rich limit where $\mu_C = \mu_C^{bulk}$, Ω of the N-type interface is 2.021 eV per unit cell of one interface, which is given by the binding energy of the N-type interface region that containing 36 Si and 37 C atomic layers in the 144-atom cell minus $36\mu_{SiC}^{bulk}$ and μ_C^{bulk}. For the Si-rich limit where $\mu_{Si} = \mu_{Si}^{bulk}$, Ω of the P-type interface is 1.815 eV per unit cell, which is given by the binding energy of the P-type interface region containing 36 Si and 35 C atomic layers in the 144-atom cell minus $35\mu_{SiC}^{bulk}$ and μ_{Si}^{bulk}.

For the allowable ranges of the atomic chemical potentials of equation (4) the thermodynamic potentials of the interfaces can be expressed as a function of the atomic chemical potentials [32] as shown in figure 6. This figure shows the relative stability between the three types of polar and non-polar interfaces of the {122} Σ = 9 boundary in SiC. This figure successfully represents the general tendency that the C-rich interface is most stable in a C-rich atmosphere, and vice versa. This figure also indicates that either one or the other polar interface is always more stable than the non-polar interface for the allowable ranges of the atomic chemical potentials. The value of Ω at the point of intersection of the two lines representing the polar interfaces is smaller than that of the non-polar interface in figure 6. This is directly caused by the result that the formation energy of the pair of polar interfaces is smaller than that of the non-polar interfaces as mentioned in section 4.

As mentioned in section 3 the calculated binding energies of the respective interface regions are significant only when the charge neutrality is preserved for the respective regions. We think that the existing transfer of 0.0007*e* between the two regions has only trivial effects, because the binding energy per electron is of the order of 1 eV in the

present case. In addition, it should be noted that another division of the cell into two non-stoichiometric regions by transferring one Si and one C atomic layers from the N-type interface region to the P-type interface region does little to change the results, because the atoms between the interfaces in the cell are almost like those in the bulk.

7. Discussion

The present results indicate that the respective polar interfaces of the $\{122\}\,\Sigma = 9$ boundary in SiC possibly exist alone, without the generation of any macroscopic electrostatic fields or free carriers. Generally, it seems that polar interfaces are possibly stable in SiC, because the wrong bonds in SiC do not generate extra carriers or deep states, and the charge neutrality can be preserved in the respective interface regions.

The present results also indicate that either one or the other polar interface is always more stable than the non-polar interface in the case of the $\{122\}\,\Sigma = 9$ boundary in SiC. This is mainly because the energy increase caused by the bond distortions is smaller at the polar interfaces containing only one type of wrong bonds than the non-polar interface containing both types of wrong bonds. However, this cannot be straightforwardly generalized to the polar and non-polar interfaces of boundaries in SiC. It is necessary to consider the difference in the total number of wrong bonds between the polar and non-polar interfaces. In the case of the $\{122\}\,\Sigma = 9$ boundary the total number of wrong bonds at the pair of polar interfaces is the same as that at the pair of non-polar interfaces. In such cases it seems that the relative stability of the polar interfaces as compared with the non-polar interface in SiC can be expected. However, in the case of the $\{111\}\,\Sigma = 3$ boundary, the non-polar interface contains no wrong bonds, although the bonds at the polar interfaces are all wrong bonds. It can be stated that the non-polar interface of the $\{111\}\,\Sigma = 3$ boundary in SiC should be more stable than the polar interfaces, because the formation energy of the wrong bond is large in SiC.

Finally, we discuss the stability of the polar interfaces of boundaries in compound semiconductors such as III–V or II–VI compounds. The wrong bonds in such compounds are either oversaturated or undersaturated and they generate extra carriers [29] differently from the wrong bonds in SiC. At the non-polar interfaces these carriers are compensated. However, these may not be compensated at the polar interfaces, which contain only one type of wrong bonds or one type of excess wrong bonds.

For the stability of the polar interfaces in heterovalent compound semiconductors, firstly, it might be important that the extra carriers are well localized near the wrong bonds by being trapped by proper states inside the gap. There emerge charge accumulation and macroscopic electrostatic fields when the extra carriers are not bounded, as discussed by Harrison *et al* for the polar interface in semiconductor heterojunctions [20]. Secondly, it might be more favourable to compensate the extra carriers by proper reconstruction as discussed by Martin [21]. It can be stated that the excess carriers caused by wrong bonds are compensated by creating defects such as dangling bonds when the energy release by compensation exceeds the defect creation energy [21, 29]. This problem of carrier compensation indicates the possibility of fairly different types of structures and properties of the boundaries in III–V or II–VI compound semiconductors as compared with those in SiC or Si. The above points seem to be important in order to understand the recent observations of boundaries in GaAs using HREM [12].

It should be noted that the present type of supercell calculation containing both types of polar interfaces in one unit cell cannot be applied to heterovalent compound

semiconductors without any modification, because transfer of extra carriers should occur between the two interfaces, unlike the case of SiC. Special schemes would be necessary in order to prevent such artificial charge transfers as were used in the case of the polar surfaces of GaAs [18, 19].

8. Conclusions

The polar and non-polar interfaces of grain boundaries in the zinc blende structure can be defined by the stoichiometry in the interface region. Polar interfaces contain one type of wrong bonds or one type of excess wrong bonds, although non-polar interfaces contain no wrong bonds or the same numbers of the two types of wrong bonds. Generally, it is possible to construct two polar and one non-polar interfaces for a symmetrical-tilt grain boundary the interface of which has polar surfaces. For the $\{122\}$ $\Sigma = 9$ boundary in SiC we have constructed the atomic models of two polar and one non-polar interfaces consisting of a zigzag arrangement of 5–7 units, which are consistent with an HREM image. The N-type polar interface contains the C—C wrong bonds and the P-type polar interface contains the Si—Si wrong bonds, although the non-polar interface contains both types of wrong bonds.

We have examined the atomic and electronic structures of the polar interface models of the $\{122\}$ $\Sigma = 9$ boundary in SiC by using the SCTB method coupled with the supercell technique, following the non-polar interface model in our previous paper. Although the supercell must contain both types of polar interfaces, the calculated structures and properties of the respective polar interface regions in the supercell can be regarded as general, because there are no significant charge transfers or interactions between the two polar interfaces in the present supercell.

The present results indicate that, as well as the non-polar interface, the respective polar interfaces possibly exist in a stable form without the generation of any charge accumulation, macroscopic electrostatic fields or excess free carriers. This is because the atomic charges in SiC are mainly caused by the bond polarization and the wrong bonds in SiC do not generate any extra carriers or deep states, unlike the ionic solids or heterovalent compound semiconductors.

For the rigid-body translation between the two grains of the $\{122\}$ $\Sigma = 9$ boundary in SiC, the N-type polar interface and the P-type polar interface are characterized by a slight compression and by a slight dilatation normal to the interface, respectively, although the non-polar interface is characterized by a translation along the $\langle 411 \rangle$ direction in addition to a slight dilatation. There is a dipole shift at the non-polar interface, although the polar interfaces contain no dipole shifts. The bond distortions are smaller at the polar interfaces containing only one type of wrong bonds rather than the non-polar interface containing both types of wrong bonds. This causes the smaller formation energy of the pair of polar interfaces as compared with that of the non-polar interfaces.

The wrong bonds at the polar interfaces generate the wrong-bond localized states at the band edges and the increase in the electrostatic energy as well as at the non-polar interface. In both the polar and non-polar interfaces the C—C wrong bonds introduce the localized states at the bottom of the valence band and above the conduction band, and the Si–Si wrong bonds introduce the localized state at the bottom of the conduction band and at the top of the valence band. In addition, there exist the states that are mainly localized at the 5–7 units at the band edges at both the polar and non-polar interfaces.

By using the calculated binding energies we have performed a thermodynamic analysis of the relative stability of the polar and non-polar interfaces of the {122} $\Sigma = 9$ boundary in SiC as a function of the atomic chemical potentials, because these interfaces have different stoichiometries. The calculated thermodynamic potentials of the interfaces indicate that the N-type interface is most stable for the C-rich atmosphere and vice versa, and that either one or the other polar interface is always more stable than the non-polar interface for the allowable ranges of the atomic chemical potentials. This is because the energy increase caused by the bond distortions is smaller at the polar interfaces.

It seems that polar interfaces possibly exist in a stable form in SiC in general. Additionally, it appears that the relative stability of the polar interfaces against the non-polar interface in SiC can be generally expected when the total numbers of wrong bonds are the same between the polar and non-polar interfaces as in the case of the {122} $\Sigma = 9$ boundary. For the stability of polar interfaces in heterovalent compound semiconductors the localization or compensation of excess carriers should, in general, be important.

Acknowledgments

All the calculations were performed on the CRAY X-MP at RIPS center of the Japanese Agency of Industrial Science and Technology. We would like to thank the staff of the RIPS center for their help in using the supercomputer. MK is grateful to Dr A P Sutton for a fruitful discussion at POLYSE '90 and for sending us a preprint of his recent publication.

References

[1] Möller H J, Strunk H P and Werner J H (ed) 1989 *Polycrystalline Semiconductors* (Berlin: Springer)
[2] Werner J H and Strunk H P (ed) 1991 *Polycrystalline Semiconductors II* (Berlin: Springer) at press
[3] Krivanek O L, Isoda S and Kobayashi K 1977 *Phil. Mag.* **36** 931
[4] d'Anterroches C and Bourret A 1984 *Phil. Mag.* A **49** 783
[5] Bourret A and Bacmann J J 1985 *Surf. Sci.* **162** 495
[6] Thibault-Desseaux J and Putaux J L 1989 *Structure and Properties of Dislocations in Semiconductors 1989 (Inst. Phys. Conf. Ser. 104)* (Bristol: Institute of Physics) p 1
Putaux J L and Thibault-Desseaux J 1990 *J. Physique Coll.* **51** C1 323
[7] Thomson R E and Chadi D J 1984 *Phys. Rev.* B **29** 889
[8] DiVincenzo D P, Alerhand O L, Schlüter M and Wilkins J W 1986 *Phys. Rev. Lett.* **56** 1925
[9] Paxton A T and Sutton A P 1988 *J. Phys. C: Solid State Phys.* **21** L481; 1989 *Acta Metall.* **37** 1693
[10] Kohyama M, Yamamoto R, Ebata Y and Kinoshita M 1988 *J. Phys. C: Solid State Phys.* **21** 3205
Kohyama M, Yamamoto R, Watanabe Y, Ebata Y and Kinoshita M 1988 *J. Phys. C: Solid State Phys.* **21** L695
Kohyama M, Kose S, Kinoshita M and Yamamoto R 1989 *J. Phys.: Condens. Matter* **1** 8251
[11] Holt D B 1964 *J. Phys. Chem. Solids* **25** 1385
[12] Cho N-H, Carter C B, Wagner D K and McKernan S 1987 *Microscopy of Semiconducting Materials 1987 (Inst. Phys. Conf. Ser. 87)* p 281
Cho N-H, McKernan S, Wagner D K and Carter C B 1988 *J. Physique Coll.* **49** C5 245
Cho N-H, Rasmussen D R, McKernan S, Carter C B and Wagner D K 1988 *Mater. Res. Soc. Symp. Proc.* **122** 33
[13] Williams J O and Wright A C 1987 *Phil. Mag.* A **55** 99
[14] Hiraga K 1984 *Sci. Rep. Res. Inst. Tohoku University* A **32** 1

[15] Ichinose H, Inomata Y and Ishida Y 1987 *Materials Science Research* vol 21, ed J A Pask and A G Evans (New York: Plenum) p 255
[16] Kohyama M, Kose S, Kinoshita M and Yamamoto R 1990 *J. Phys.: Condens. Matter* **2** 7809
[17] Kohyama M, Kose S, Kinoshita M and Yamamoto R 1990 *J. Phys.: Condens. Matter* **2** 7791
[18] Kaxiras E, Bar-Yam Y, Joannopoulos J D and Pandey K C 1987 *Phys. Rev.* B **35** 9625; B **35** 9636
[19] Qian Guo-Xin, Martin R M and Chadi D J 1988 *Phys. Rev. Lett.* **60** 1962; 1988 *Phys. Rev.* B **38** 7649
[20] Harrison W A, Kraut E A, Waldrop J R and Grant R W 1978 *Phys. Rev.* B **18** 4402
[21] Martin R M 1980 *J. Vac. Sci. Technol.* **17** 978
[22] Landau L D and Lifshitz E M 1958 *Statistical Physics* (London: Pergamon)
[23] Sutton A P 1991 *Polycrystalline Semiconductors II* ed J H Werner and H P Strunk (Berlin: Springer) at press
[24] Kohyama M, Yamamoto R and Doyama M 1986 *Phys. Status Solidi* b **137** 11
Kohyama M 1987 *Phys. Status Solidi* b **141** 71
[25] Holt D B 1969 *J. Phys. Chem. Solids* **30** 1297
[26] Hagège S, Shindo D, Hiraga K and Hirabayashi M 1990 *J. Physique Coll.* **51** C1 167
[27] Majewski J A and Vogl P 1987 *Phys. Rev.* B **35** 9666
[28] Kohyama M, Yamamoto R, Ebata Y and Kinoshita M 1989 *Phys. Status Solidi* b **152** 533
[29] O'Reilly E P and Robertson J 1986 *Phys. Rev.* B **34** 8684
[30] Lambrecht W R L and Segall B 1990 *Phys. Rev.* B **41** 2948
[31] Wang C, Bernholc J and Davis R F 1988 *Phys. Rev.* B **38** 12752
[32] Northrup J E 1989 *Phys. Rev. Lett.* **62** 2487